ACS OMEGA

http://pubs.acs.org/journal/acsodf

Article

Spidroin Silk Fibers with Bioactive Motifs of Extracellular Proteins for Neural Tissue Engineering

Veronica A. Revkova,* Konstantin V. Sidoruk, Vladimir A. Kalsin, Pavel A. Melnikov, Mikhail A. Konoplyannikov, Svetlana Kotova, Anastasia A. Frolova, Sergey A. Rodionov, Mikhail M. Smorchkov, Alexey V. Kovalev, Alexander V. Troitskiy, Peter S. Timashev, Vladimir P. Chekhonin, Vladimir G. Bogush, and Vladimir P. Baklaushev

Cite This: *ACS Omega* 2021, 6, 15264−15273

Read Online

ACCESS | Metrics & More | Article Recommendations | Supporting Information

ABSTRACT: The interaction of neural progenitor cells (NPCs) with the extracellular matrix (ECM) plays an important role in neural tissue regeneration. Understanding which motifs of the ECM proteins are crucial for normal NPC adhesion, proliferation, and differentiation is important in order to create more adequate tissue engineered models of neural tissue and to efficiently study the central nervous system regeneration mechanisms. We have shown earlier that anisotropic matrices prepared from a mixture of recombinant dragline silk proteins, such as spidroin 1 and spidroin 2, by electrospinning are biocompatible with NPCs and provide good proliferation and oriented growth of neurites. This study objective was to find the effects of spidroin-based electrospun materials, modified with peptide motifs of the extracellular matrix proteins (RGD, IKVAV, and VAEIDGIEL) on adhesion, proliferation, and differentiation of directly reprogrammed neural precursor cells (drNPCs). The structural and biomechanical studies have shown that spidroin-based electrospun mats (SBEM), modified with ECM peptides, are characterized by a uniaxial orientation and elastic moduli in the swollen state, comparable to those of the dura mater. It has been found for the first time that drNPCs on SBEM mostly preserve their stemness in the growth medium and even in the differentiation medium with brain-derived neurotrophic factor and glial cell line-derived neurotrophic factor, while addition of the mentioned ECM-peptide motifs may shift the balance toward neuroglial differentiation. We have demonstrated that the RGD motif promotes formation of a lower number of neurons with longer neurites, while the IKVAV motif is characterized by formation of a greater number of NF200-positive neurons with shorter neurites. At the same time, all the studied matrices preserve up to 30% of neuroglial progenitor cells, phenotypically similar to radial glia derived from the subventricular zone. We believe that, by using this approach and modifying spidroin by various ECM-motifs or other substances, one may create an *in vitro* model for the neuroglial stem cell niche with the potential control of their differentiation.

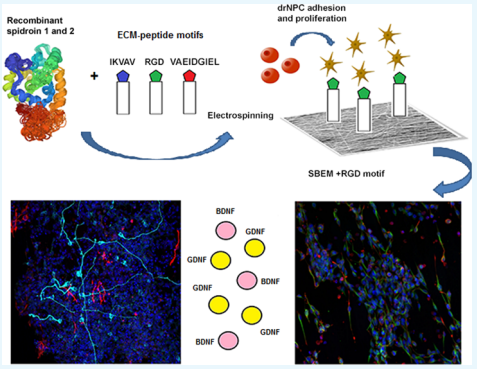

INTRODUCTION

Neural tissue represents one of the most sophisticated objects both from the viewpoint of obtaining and culturing certain cell types and from the viewpoint of creating organotypic models, in which different cell types interact with each other and with the extracellular matrix (ECM).[1]

Appearance of technologies for cell reprogramming, which allow one to obtain human neural and glial progenitors from somatic cells,[2,3] has essentially simplified the task of preparing cultures of the neural tissue cells. Neural progenitor cells obtained by direct reprogramming (drNPCs) show great promise for the creation of neuro-regenerative technologies. In contrast to induced pluripotent stem cells (iPSC) derivatives, drNPCs may be obtained much faster,[4] prospectively even *in situ*, which will allow avoiding the risks of *ex vivo* culturing,[5] and they are not genomically unstable and not tumorigenic.[2] At the same time, their interaction with the microenvironment and specifics of 3D culturing are understood poorer than those of iPSC derivatives. The development of ECM-mimicking biomaterials has made it possible to create organotypic 3D cultures for studying directed differentiation, migration, and intercellular cooperation of neuroglial cells.[6,7]

Recombinant spidroin has been extensively studied as a biomaterial with a high potential in the field of the central nervous system (CNS) damage repair.[8] It is known that the tensile strength of the native dragline silk fibers is almost as

Received: March 24, 2021
Accepted: May 12, 2021
Published: May 30, 2021

high as the strength of steel, while their breaking elongation is five times higher than that of a tendon.[9] Such indices are achieved due to the unique structure of dragline silk, determined mainly by long repeated amino acid sequences.[10] Due to the presence of the Arg-Glu pair at both the N- and C-termini, spidroins may form dimers, thus stabilizing their structure. Most spiders have two native types of spidroin: spidroin 1 and spidroin 2 (Major ampullate Spidroin I and Spidroin 2). Creation of recombinant spidroins equivalent to the native forms provides preparation of proteins with similar mechanical properties. The ability of spidroins to self-assemble is widely used in the development of various biomaterials such as micro- and nanocapsules, hydrogels, fibers, films, tubes, and electrospun mats.[8]

In our previous study, we have shown that spidroin-based electrospun mats (SBEM) together with platelet-rich plasma (PRP) may find application in the engineering of neural tissue. Recombinant spidroin contains 18 repeats of the GRGGL motif, which is recognized by the NCAM protein and provides good adhesion and oriented growth of neuronal progenitors.[6] The tissue engineered construct based on SBEM and PRP has shown high biocompatibility with the damaged spinal cord tissue in primates. In addition, such an organotypic 3D construct sustained the survival of transplanted drNPCs for no less than 12 weeks post-transplantation.

The technique for the preparation of recombinant spidroins allows their easy modification, e.g., by means of embedding ECM proteins to mimic the cell microenvironment. It has been demonstrated in a number of studies that inclusion of motifs of ECM peptides, such as RGD (fibronectin mimetic peptide,) IKVAV (laminin mimetic peptide), and VAEIDGIEL (tenascin-C mimetic peptide), into the structure of different biomaterials significantly enhances adhesion, proliferation, and growth of neuroglial cells and their processes.[11−16] In particular, the incorporation of the RGD motif in biomaterials provides more active neuritis growth and enhanced synaptic signaling.[17] IKVAV is assumed to stimulate reprogramming of mesenchymal stem cells in the neuronal direction.[14,18] The photoactivated form of IKVAV, IK(HANBP)VAV, provides light-guided axon growth *in situ*.[19,20] For tenascin-C, it was shown that it modulates cell cycle length and differentiation in neural stem/progenitor cells and participates in the formation of the radial glia type B of the adult CNS stem cell niches.[21,22] However, it remains unclear how these proteins and their active peptides influence on drNPC differentiation.

The interaction of ECM proteins with cells is realized through the membrane receptors on the surface of cells: integrins, neuropilin, etc. RGD binds to integrins $\alpha5\beta1$, $\alpha5\beta3$, and $\alpha5\beta5$;[23] IKVAV to integrins $\alpha3\beta1$, $\alpha4\beta1$, and $\alpha6\beta1$;[24] VAEIDGIEL, to integrins $\alpha5\beta3$, $\alpha5\beta6$, $\alpha7\beta1$, $\alpha8\beta1$, and $\alpha9\beta1$.[16] The survival of cells contacting with such integrin-binding peptides essentially increases even in the absence of growth factors.[11,14] On the other hand, the ECM-peptide motifs may attract and accumulate growth factors due to the binding of receptors of growth factors to the ECM receptors.[25] The ECM proteins together with growth factors also induce the intracellular signal transfer via cell surface receptors.[26]

The objective of this study was to elucidate the effects of SBEM, modified with peptide motifs of the ECM proteins, fibronectin (RGD), laminin (IKVAV), and tenascin-C (VAEIDGIEL), on proliferation, self-renewal, and differentiation of drNPCs.

RESULTS

Morphology and Biomechanics of SBEM, Modified with ECM-Peptide Motifs. Scanning electron microscopy (SEM) images (Figure 1) of SBEM clearly demonstrate their anisotropic structure, with a predominantly uniaxial orientation of fibers. The fibers are rather tightly packed; however, their reticulate 3D structure is uncovered at higher-resolution AFM images.

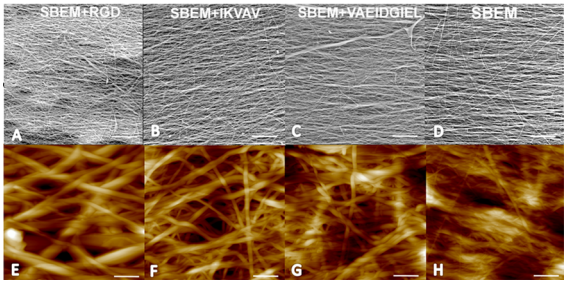

Figure 1. Scanning electron microscopy (A−D) and atomic force microscopy (E−H) of the SBEM functionalized by ECM-peptides RGD (A, E), IKVAV (B, F), and VAEIDGIEL (C, G). (D, H) Non-modified SBEM. Bar size = 30 μm (A−D), 5 μm (E−H).

The continuous 3D network of spidroin fibers is interrupted by gaps, with the dimensions of one to several microns. The latter may appear favorable for the growth of cell sprouts. The addition of the studied peptide motifs did not affect the ultrastructure and anisotropic properties of the prepared SBEM. Nevertheless, the diameter of fibers significantly increased after the addition of the ECM-peptide motifs, from 117 ± 45 nm for the control SBEM to 178 ± 60 nm and 171 ± 41 nm for SBEM-IKVAV and SBEM-VAEIDGIEL, respectively, and reached the highest 339 ± 157 nm for RGD (Figure S1). At the same time, the thickness of films did not significantly differ and is measured to be 10−12 μm (Table S1).

The biomechanical properties of SBEM were characterized by their Young's moduli measured by atomic force microscopy (AFM) (Table 1). The Young's modulus of dry samples was 1.6 GPa for all the studied mats, unmodified and modified with different motifs. The observed Young's moduli indicate a high stiffness of spidroin fibers packed in a 3D network in SBEM, comparable to that of spidroin fibers stretched along the fiber direction.[27,28] In the aqueous medium, spidroin fibers swell, and the Young's modulus of scaffolds drops to megapascals (Table 1).

Table 1. Young's Moduli (on Air and in Water) of Spidroin-Based Mats Modified with the ECM Proteins' Motifs[a]

	Young's modulus (GPa)	Young's modulus (MPa)
sample name	dry	swollen
SBEM+RGD	1.6 ± 0.2	1.7 ± 0.3
SBEM+IKVAV	1.6 ± 0.4	10.6 ± 3.0[a]
SBEM+VAEIDGIEL	1.6 ± 0.1	0.7 ± 0.3
SBEM	1.6 ± 0.2	1.5 ± 0.3

[a]Designations: SBEM, recombinant spidroin-based electrospun mat. RGD, IKVAV, VAEIDGIEL, ECM-peptide motifs of fibronectin, laminin, and tenascin-C, respectively. *p < 0.01 when compared to control.

https://doi.org/10.1021/acsomega.1c01576
ACS Omega 2021, 6, 15264−15273

Interestingly, the swollen scaffolds differed in their mechanical properties, in contrast to the dry samples. The IKVAV-SBEM was the stiffest scaffold with the Young's modulus of 10.6 ± 3.0 MPa, while the VAEIDGIEL-SBEM was the softest one (0.7 ± 0.3 MPa), two times softer than the unmodified spidroin sample.

Cell Adhesion and Proliferation. drNPCs exhibited high adhesive properties toward all the types of spidroin matrices. This finding is in a good agreement with the previously reported data on the compatibility of anisotropic mats prepared from a mixture of recombinant spidroins with drNPCs due to the presence of the GRGGL motif recognized by NCAM 6. At the stage of adhesion and subsequent proliferation, the embedded additional motifs led to formation of conglomerates by drNPCs in the case of RGD and IKVAV motifs and drNPC proliferation in the form of attached cytospheres (Figure 2A,B). In the control SBEM and those containing the tenascin-C VAEIDGIEL motif, cells were distributed over the mats' surface more uniformly (Figure 2C).

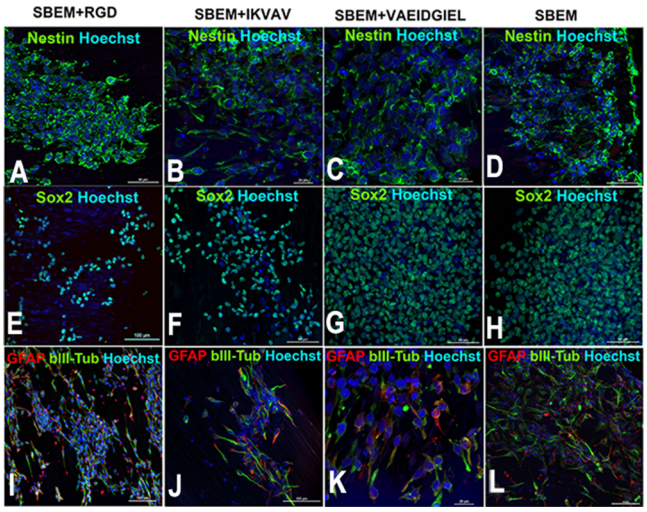

Figure 2. Proliferation of drNPCs on the SBEM with or without the ECM-peptide motifs in the growth medium. drNPCs on all the SBEM intensively expressed Nestin (A−D), whereas the percentage of SOX2-positive cells (E−H) and the co-expression of βIII-tubulin and GFAP (I−L) were significantly higher in the control group. The cells were stained with cocktails of primary antibodies (mouse monoclonal + rabbit polyclonal) followed by cocktail of goat-anti-mouse and goat-anti-rabbit secondary antibodies with Alexa Fluor 488 (green) and Alexa Fluor 633 (red), respectively. The cell nuclei were stained with Hoechst (blue) in all the panels. Laser scanning confocal microscopy. Bar size = 20−100 μm.

During 10 day-long culturing in the growth medium, the expression of the basic NPC markers, such as Nestin and SOX2, was observed in all the samples (Figure 22E−HA−D and Figure , respectively). The number of Nestin-positive cells, according to the flow cytometry data, made more than 95% from the total number of cells in all the samples (Table S2). The SOX2 expression in the growth medium was observed in almost 100% (99.3 ± 0.1%) of cells in the control samples without the motifs, according to the flow cytometry data. For matrices with the RGD and IKVAV motifs, only 63.0 ± 1.4% and 66.7 ± 2.0% of cells, respectively, were SOX2-positive. SBEM with the VAEIDGIEL motif, although not differing from the control matrices visually, showed only 62.5 ± 1.8% of SOX2-positive cells by flow cytometry (Figure 5A, dark columns).

In our previous reports, we demonstrated that drNPCs, similar to embryonic neural stem cells (H9-ESC-NSCs) and stem cells of the subventricular zone of the adult brain, co-expressed a pro-neuronal marker, βIII-tubulin, and a protein of glial intermediate filaments, GFAP.[6,7] This co-expression is observed up to the start of differentiation toward terminal subtypes and may serve as an indicator of drNPCs' stemness. The fraction of cells co-expressing βIII-tubulin and GFAP in the growth medium in the control containing spidroins only was 93.2 ± 3.4%, which testifies that almost all drNPCs sustained their stemness. In SBEM with the IKVAV motif, the co-expression of βIII-tubulin and GFAP was observed only in 70.3 ± 1.6%, while in mats with the VAEIDGIEL and RGD motifs, it was 65.6 ± 3.0% and 61.2 ± 1.8%, respectively, which likely reflected a phenomenon of spontaneous differentiation on SBEM with the mentioned motifs. At the same time, no significant increase in the GFAP-only-positive or βIII-tubulin-only-positive cells' fraction was observed (Figure 5B,C, dark columns), which indicated the absence of terminally differentiated cell elements.

Thus, the addition of specific motifs of the ECM proteins to the matrix based on recombinant spidroins does not impair the intrinsic adhesive properties of spidroin. It also stimulates spontaneous formation of intermediate cell types from drNPCs, SOX2-negative, and not co-expressing GFAP and βIII-tubulin.

Cell Differentiation. To create tissue engineered constructs for transplantation into the region of the brain or spinal cord damage, it is important to sustain a balance between the degree of stemness of the transplanted cells (since terminally differentiated cell types will unlikely survive transplantation) and their ability to differentiate in the direction targeted for a certain structure. To study the effect of SBEM on the neuronal-glial differentiation, after 3 days of culturing in the growth medium, we replaced bFGF and epidermal growth factor (EGF) with the differentiation growth factors [brain-derived neurotrophic factor (BDNF) and glial cell line-derived neurotrophic factor (GDNF)] and continued growing for 10 more days (Figure 3).

The immunocytochemical study conducted after culturing in the differentiation medium showed that the expression of the progenitor marker, Nestin, still remained as high as 90% for all the samples (Figure 3A−D). The number of SOX2-positive cells (79.3 ± 0.3% in the differentiation medium) in the control matrices almost did not change, as compared to that in the growth medium (Table S2). This finding testifies the preservation of stemness by the majority of cells, in spite of the presence of GDNF and BDNF. The presence of RGD, IKVAV, and VAEIDGIEL motifs under differentiation conditions unidirectionally influenced the SOX2 expression, decreasing it dramatically (Figures 3 and 5A). Simultaneously, on all the peptide-containing mats, we observed a decrease in the number of cells co-expressing βIII-tubulin and GFAP, with their substitution by subpopulations of cells expressing these markers separately (Figures 3E−H and 5D). In all the cases, GFAP-positive astrocytes dominated, but their highest number was formed on mats with the RGD motif (52.8 ± 3.5%), while for IKVAV and VAEIDGIEL-containing SBEM, the astrocyte number was 32.2 ± 1.0% and 27.2 ± 1.5, respectively (Figure 5B). The number of cells expressing only βIII-tubulin was 1.4

https://doi.org/10.1021/acsomega.1c01576
ACS Omega 2021, 6, 15264−15273

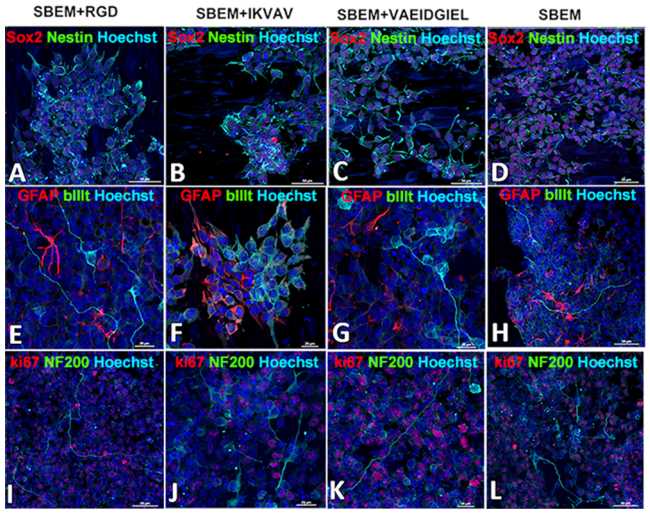

Figure 3. Differentiation of drNPCs on the SBEM with or without motifs in the medium containing BDNF and GDNF. More than 90% of drNPCs are Nestin-positive (A–D). Single cells that are only βIII-tubulin or GFAP-positive are noted (E–H). Proliferation and stemness of drNPCs supported by Ki-67 (I–L). Long neurites are revealed using NF200 (I–L). The secondary antibodies and nuclei staining are the same as in Figure.2. Laser scanning confocal microscopy. Bar size = 50 μm.

± 0.1%, 2.3 ± 0.1%, and 0.8 ± 0.1% for the RGD, IKVAV, and VAEIDGIEL motifs, respectively (Figure 5C).

The fact that some fraction of drNPCs underwent neuronal differentiation was also verified by staining for NF-200, which revealed the presence of positive cells with long neurites on SBEMs containing the ECM-peptide motifs (Figure 3I–L). The fraction of those cells did not significantly change from one type of SBEM to another and did not exceed 2%; however, the length of neurites depended on the peptide type. The longest neurites (up to 400 μm) formed on SBEMs containing the RGD motif of fibronectin, the median of their length being 106.9 ± 80.75 μm (Figure 4A–D). In the control SBEM and in the SBEM with the laminin peptide motif (IKVAV), the length of neuritis was significantly lower at 26.3 ± 10.9 and 40.1 ± 16.95 μm, respectively. The length of neuritis in SBEM with the tenascin-C motif (VAEIDGIEL) was intermediate (83.0 ± 64.77 μm).

In the process of asymmetric division and differentiation of NSCs in general and drNPCs in particular, cell death is observed.[4,29] Fragments of dead cells remain attached to spidroin fibers that is clearly revealed by Hoechst staining and SEM (Figure 5B). When stained for GFAP and βIII-tubulin, a large number of cells surrounding astrocytes and neurons were negative with respect to both markers after differentiation (Figure 3E–H).

This fact led us to a suspicion that all negative cells may be dying cells in the state of apoptosis. To exclude that and to analyze the proliferative activity of cells in the differentiation medium, we applied additional staining for Ki-67 (Figure 3I–L). The staining showed that the proliferative index was very high in all the specimens (higher than 50%), i.e., GFAP- and βIII-tubulin-negative cells were viable and probably presented some intermediate forms of progenitors.

In total, all the described data indicate the initiation of differentiation on SBEMs with the ECM-peptide motifs, both in proliferative and differentiative media, and the differentiation being mostly glial. In a small cell fraction (not exceeding 2% of the total cell number), which underwent neuronal differentiation, the longest neurites formed on SBEM with the RGD motif. At the same time, up to 30% of cells in the differentiation medium preserved the signs of stemness and

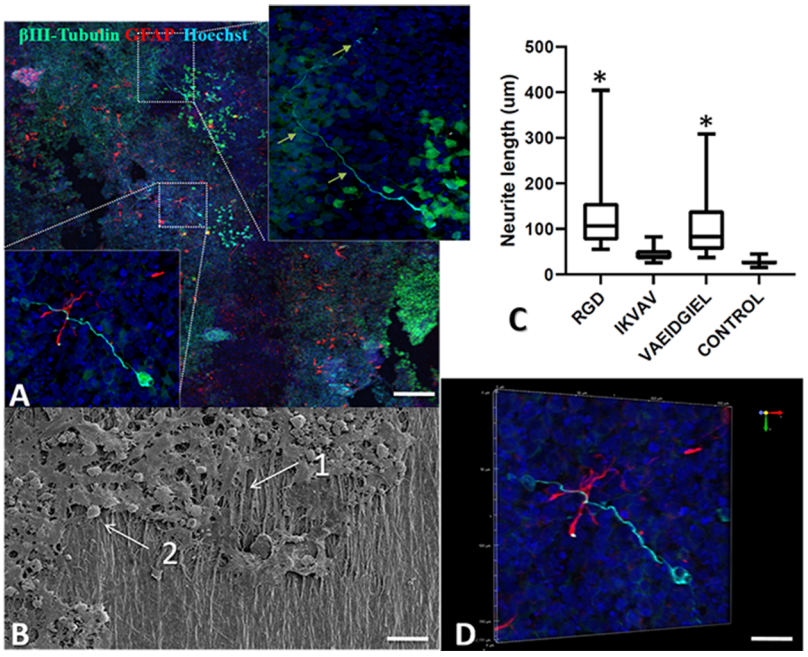

Figure 4. Examples of drNPC differentiation on SBEM+RGD. (A) Staining with βIII-tubulin (green), GFAP (red), and Hoechst (blue). Bar size = 200 μm; enlarged panels demonstrate neurons with long neurites (shown by green arrows). (B) Scanning electron microscopy. Bar size = 100 μm. Arrow 1 shows a neurite oriented along the spidroin fibers. Arrow 2 shows an apoptotic cell. (C) Neurite length histogram (median, min, max, and 25% and 75% percentiles). *p < 0.01 as compared with control. (D) A three-dimensional reconstruction shows a neuron with a long neurite interacting with an astroglial cell. Bar size = 50 μm.

https://doi.org/10.1021/acsomega.1c01576
ACS Omega 2021, 6, 15264–15273

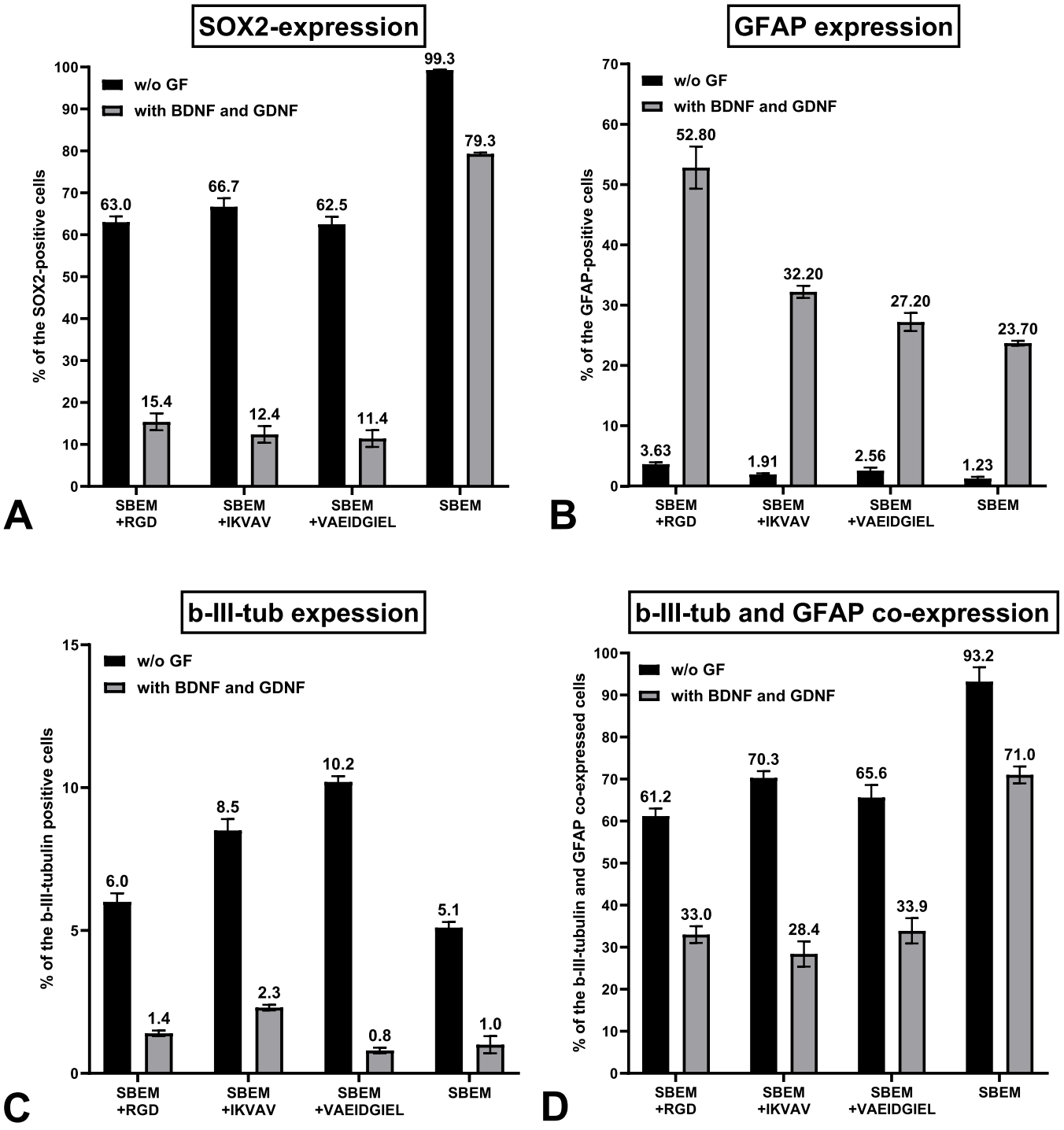

Figure 5. Immunophenotyping assay of drNPCs cultured on the SBEM with or without the ECM-peptide motifs. (A) Percent of the SOX2-positive cells in spontaneous and induced differentiation of the drNPCs. (B, C) Number of cells, which expressed only GFAP$^+$ and βIII-tubulin$^+$ markers after spontaneous and induced differentiation. (D) Amount of the drNPCs, which co-expressed the neural and glial markers.

continued to proliferate, according to staining for Ki-67, on all the spidroin matrices.

DISCUSSION

ECM-peptide motifs have long been utilized in the creation of scaffolds for neural tissue cells as components of biomaterials (see refs 30 and 31 for review). In our study, we were interested in the ECM-peptide motifs' influence on the behavior of cells seeded on spidroin mats, which proved themselves advantageous in tissue engineering.[6]

We have shown that all the SBEM, both the unmodified ones and those with added peptides, become softer by 2−3 orders of magnitude upon swelling. The Young's moduli of most of SBEM in the aqueous medium, measuring 1−2 MPa, correspond to the elastic modulus of the dura mater of the spinal cord.[32] However, SBEM-IKVAV has a notably higher Young's modulus in the swollen state than the other SBEM. The reason for this peculiar behavior is not completely clear. A possible explanation may be associated with the interior packing of spidroin macromolecules in fibers during electro-

https://doi.org/10.1021/acsomega.1c01576
ACS Omega 2021, 6, 15264−15273

spinning. The three used motifs have amino acid sequences, which differ essentially in the distribution of charges and hydrophobicity. The IKVAV motif is essentially hydrophobic, which may provide its higher affinity to spidroin containing long polyalanine and glycine-rich sequences. Thus, the presence of IKVAV probably leads to denser packing of spidroin moieties in a fiber and a correspondingly higher stiffness. Given the size of the AFM tip (20 nm), it is the stiffness of spidroin fibers and their bundles that mostly contributes to the measured Young's modulus. This difference is not noticeable in the dry state since the 3D network of spidroin is rather compact, but it is observable in the much looser 3D network of swollen fibers. The difference in the interior packing density during electrospinning is likely responsible for the increase in the thickness of fibers in the presence of all the motifs in comparison with the control SBEM and in particular for unusually thick fibers in SBEM-RGD. However, taking into account that no difference was found in adhesion and proliferation of drNPCs on SBEM-IKVAV and other matrices, we may conclude that the almost tenfold difference in the Young's modulus did not essentially affect the cells' behavior.

In general, we believe the obtained results of biomechanical study to be satisfactory since such constructs are suggested for the use in the spinal cord regeneration, e.g., in the form of a patch placed in the projection of a cyst, directly below the dura mater, with a possibility of sewing the patch to the latter. The anisotropy inherent to spidroin creates a peculiar orienting "railway" for migration and growth of NPC sprouts attempting to get over the lesion.

The choice of recombinant spidroin for the creation of anisotropic mats is stipulated by the presence of the GRGGL sequence in its composition, which is recognized by NCAM and provides good adhesion of neural progenitors to mats. The RGD (fibronectin mimetic), IKVAV (laminin mimetic), and VAEIDGIEL (tenascin-C mimetic) motifs were chosen since all of them were shown to affect NPC proliferation and/or differentiation.[13,21] The molar ratio of ECM-peptide motifs:spidroin = 20:1 was selected due to the 18 repeats of the GRGGL motif in the amino acid sequence of spidroin. Thus, we tried to prepare the equimolar ratio of the GRGGL motif and ECM-peptide motif. All the SBEM had a similar thicknesses of 10−12 μm.

drNPCs were shown earlier to be multipotent and capable of differentiation in three basic directions: neuronal, astrocytic, and oligodendrocytic.[1] Such a potential to differentiation is extremely important for the repair of the CNS damage. The drNPC interaction with the ECM proteins, as well as with growth factors, allow us to determine the direction of differentiation of these cells. An interesting finding of this study is the ability of SBEM, both unmodified and peptide-modified, to provide the preservation of undifferentiated drNPCs even in the differentiation medium. Indeed, in matrigel, in the medium containing BDNF and GDNF, in 2 weeks, almost all drNPCs undergo differentiation, characterizing by the disappearance of SOX2 and formation of a NF-200-positive neuronal network and GFAP-positive astrocytes.[7]

The same drNPCs in the same medium, seeded on SBEM without motifs, in 2 weeks, demonstrated the expression of SOX2 and co-expression of βIII-tubulin and GFAP in 70% of cells that testifies the preservation of stemness in the control group. A spidroin matrix containing the GRGGL motif is probably capable of retarding the differentiation of drNPCs on its own. On the other hand, the addition of the RGD, IKVAV, and VAEIDGIEL motifs decreased the number of cells carrying the stem/progenitor properties in the differentiation medium with BDNF and GDNF to 11−15%, as judged by the SOX2 expression, and to 28−34%, as judged by the co-expression of βIII-tubulin and GFAP. At the same time, judging by the isolated expression of GFAP and βIII-tubulin, predominantly glial differentiation was observed (the neurons to astrocytes ratio oscillated between 1:39 and 1:34 for RGD and VAEIDGIEL, respectively, to 1:14 for IKVAV). In other words, an apparent shift of the balance occurs toward the differentiation and formation of neuroblasts/neurons. It is of interest that RGD-containing matrices promoted the formation of the longest neurites compared to other substrates, which is probably related to the activating effect of RGD-binding integrins on the growth of neurites.[33,34]

The discovered phenomena allow a conclusion that differentiation of neuroglial progenitors in the 3D conditions on SBEM containing the ECM peptide motifs essentially differ from the 2D differentiation conditions on a flat surface coated with matrigel (even taking into account the fact that matrigel contains a large number of ECM proteins, hence all the ECM peptide motifs utilized in this study). The RGD motif promotes formation of a lower number of neurons with longer sprouts, and the IKVAV motif is characterized by formation of a greater number of neurons with shorter processes. In all the cases, approximately one-third of cells preserved their stemness. The stemness preservation on matrices prepared from recombinant spidroin may be both a favorable property due to reproducing the stem cell niche and providing the drNPC's survival after their transplantation into the damaged CNS region, and a negative property in the case the inhibition of differentiation is irreversible. The data of this study are insufficient to establish the formation of a stem cell niche with the sustained neurogenesis on SBEM. However, an almost unlimited opportunity to introduce various peptide motifs into recombinant spidroin makes this platform very flexible and promising from the viewpoint of further studying the neurogenesis *in vitro*. The mechanisms of the differentiation inhibition in approximately one-third of drNPCs on SBEM deserve a separate study.

CONCLUSIONS

Spidroin-based electrospun mats, modified with RGD, IKVAV, and VAEIDGIEL ECM-peptide motifs, are characterized by the biomechanical properties suitable for *in vitro* and *in vivo* experiments and represent a good substrate for drNPCs, providing their adhesion, proliferation, and differentiation. It has been found that drNPCs on spidroin matrices preserve their stemness in the growth medium and even in the differentiation medium with BDNF and GDNF, while addition of the mentioned ECM-peptide motifs may shift the balance toward neuroglial differentiation. The obtained data may be used in the creation of a model for the neuroglial stem cell niche.

MATERIALS AND METHODS

Biosynthesis of the Recombinant Spidroins. The yeast biomass growth of *S. cerevisiae* SCR-702T-1F9 and SCR-702T-2EI2 and the extraction and purification of the 2.04 g/L recombinant spidroins rS1/9 and 1.2 g/L rS2/12 were conducted as previously described.[35] Briefly, the yeast cells

https://doi.org/10.1021/acsomega.1c01576
ACS Omega 2021, 6, 15264−15273

were grown in a 3 L fermenter in YPD medium (2% of fermentative peptone (GOST 13805-76) and 1% of the yeast extract (Hefe-extract, Serva)) in the presence of 2% glucose at 30 °C for 4 days. To obtain the target proteins, 0.5 kg of the wet biomass was suspended in a lysis buffer (0.05 M sodium phosphate, pH 7.4; 0.001M EDTA; 5% glycerol) and the cells were lysed with glass beads in a MS_3 flow mill for 1.5 h; the prepared suspension was centrifuged, and the target protein was extracted from the precipitate with a 10% solution of lithium chloride in 90% formic acid with continuous stirring for 18 h followed by centrifugation. The supernatant was dialyzed against a 10 mM sodium acetate solution at pH 4.0 and clarified by centrifugation. The final purification was conducted by ion-exchange chromatography using a HiPrep 16/10 SP FF (GE Healthcare) column and an ACTApurifier (GE Healthcare) chromatograph with pH exchange (pH 4.0−pH 7.0−pH 4.0). The protein was eluted with a NaCl concentration gradient, dialyzed against deionized water, frozen at −70 °C, and freeze-dried.

Preparation of Anisotropically Structured SBEM. To prepare spinning solutions, we used 1,1,1,3,3,3-hexafluoro-2-propanol (Fluka Chemie GmBH, Germany) as a solvent. PCL (1% of 400 kDa, Biopolymer, Ukraine) was added to the mixture to improve its spinnability. The following solutions were used for the preparation of SBEM: rSp1/9 (6 wt %), rSp2/12 (1 wt %), and PCL (1 wt %). The MAPTRix-F-RGD fibronectin mimetic (#161052K, 2.5 mg), MAPTRix-L-IKVAV laminin mimetic (#162242K, 2.5 mg), and MAPTRix-M-VAEIDGIEL tenascin-C mimetic (#168312K, 2.5 mg) peptide motifs were added to the corresponding mixtures in the molar ratio of 20:1 (rSp1/9:peptide). All the MAPTRIX-peptides were acquired from Sigma-Aldrich Inc. The stable inclusion of the ECM peptides' motifs was shown by biotinylation and covalent binding to the TRITC dye (Figures S4−S6).

Electrospun mats were prepared using a NANON-01A electrospinning device, equipped with a standard spinneret and a drum collector of 100 mm in diameter. The process was conducted at the following working parameters: the rate of the spinning solution feed of 0.4 mL/h, the capillary-collector distance of 10 cm, the voltage of 9.5 kV, and the rate of the drum rotation of 1000 rpm. When the process was finalized, the prepared material was incubated in 96% ethanol for 15 min and then dried for 18 h at room temperature in a laminar flow hood. The SBEM thickness varied from 10 to 12 μm in the dry state and did not depend on the presence of added peptides (see Table S1).

Preparation of Human Neural Precursor Cells and Differentiation of Cells. Directly reprogrammed human neural progenitor cells (drNPCs) were kindly provided by New World Laboratories, Inc. (Laval, QC). drNPCs were obtained by direct reprogramming from human bone marrow-derived mononuclear cells, using a cocktail of three factors: Musashi-1 (Msi1), Neurogenin-2 (Ngn2), and methyl-CpG binding domain protein 2 (MBD2).[1] The cells were maintained in the NeuroCult-NS-A Proliferation kit medium (#05750 and #05753, StemCell Technologies, Canada) with addition of 1% B27 (#17504044, Gibco, USA), 20 ng/mL epidermal growth factor (EGF) (#713008, Biolegend, USA), and 40 ng/mL fibroblast growth factor-2 (FGF2) (#571506 Biolegend, USA) on a 1:200 matrigel coated tissue culture dish (TPP, Switzerland) in a humidified 5% CO_2, 5% O_2-filled incubator at 37 °C.[1,36] The growth medium was replaced every 2 days, and the cells were passaged at a ratio of 1:3 after 4 days. Before seeding on SBEM, the cells were detached by Accutase (#07920, StemCell Technologies, Canada) and resuspended to obtain a homogeneous suspension. Next, the cells were centrifuged at 250g for 3 min at 22 °C and seeded on SBEM (0.5 × 0.5 cm) with the coverage of 1 × 10^6 cells/SBEM or 4 × 10^6 cells/cm^2. The cells were not re-passaged on the SBEM. Spontaneous differentiation was detected on day 11 by the immunocytochemistry and flow cytometry assays.

For induced differentiation after 3 days of drNPC proliferation on SBEM, the culture medium was replaced with the NeuroCult-NS-A Proliferation kit (#05750 and #05753, StemCell Technologies, Canada), 1% B27 (#17504044, Gibco, USA), 1% CultureOne (#A3320201, Gibco, USA), 40 ng/mL BDNF (#130-096-286, Miltenyi Biotec, Germany), and 20 ng/mL GDNF (#130-098-449, Miltenyi Biotec, Germany). The medium was replaced every 3 days. Induced differentiation was detected on day 14 by the immunocytochemistry and flow cytometry assays.

Immunocytochemical Analysis. The expression of neural stem cell and neuronal and glial markers was performed by immunocytochemical analysis. The cells were fixed by adding a 4% buffered formaldehyde solution containing 0.1% saponin. Primary antibodies to mouse anti-Nestin (#MAB1259, R&D, 2 μg/mL), mouse anti-SOX2 (#560291, BD Biosciences, 5 μg/mL), mouse anti-βIII-tubulin (#MAB1195, R&D, 2 μg/mL), mouse anti-NF-200 (#N2912, Sigma-Aldrich, 5 μg/mL), rabbit anti-Ki-67 (#ab15580, Sigma-Aldrich, 5 μg/mL), and rabbit anti-GFAP (#Z0334, DAKO, 5 μg/mL) were used together with Alexa Fluor 488 goat anti-mouse IgG (H + L) or Alexa Fluor 568 goat anti-mouse IgG (H + L), and Alexa Fluor 633 goat anti-rabbit IgG (H + L) secondary antibodies (all 1:400, Invitrogen, USA). The cell nuclei were stained with Hoechst 33342 (#H3570, Thermo Fisher Scientific). Immunofluorescence was analyzed using a Nikon A1 scanning laser confocal microscope (Nikon Co., Japan). All the staining studies were conducted in series, with four repeats in each series.

Flow Cytometry Analysis. For the flow cytometry analysis, drNPCs were cultured on SBEM with/without growth factors for 10−13 days. Prior to the analysis, the cells were dissociated using Accutase (#07920, StemCell Technologies, Canada) and fixed with 4% buffered formaldehyde. Then, the cells were washed thrice with DPBS containing 1% fetal goat serum. Unlabeled primary mouse anti-βIII-tubulin (#MAB1195, R&D, 2 μg/mL) and rabbit anti-GFAP antibodies (#Z0334, DAKO, 5 μg/mL) incubated with Alexa Fluor 488-labeled or Alexa Fluor 568 goat anti-mouse IgG (H + L) and Alexa Fluor 633-labeled secondary antibodies (all 1:400, Invitrogen) were used for staining the cells. PE-conjugated mouse anti-SOX2 (SOX2, #560291, BD Biosciences, 5 μg/mL) antibodies were also used. The analysis was performed with a MACS Quant 16X cytometer (Myltenyi Biotec) using the Partec FloMax flow cytometry Data Acquisition and Analysis Software.

Atomic Force Microscopy Studies. The AFM imaging and mechanical studies of spidroin scaffolds were performed with a Bioscope Resolve atomic force microscope (Bruker, USA).

The AFM imaging and mechanical studies on air were conducted using rectangular silicon RTESPA-150 cantilevers with a nominal spring constant of 5 N/m, a nominal frequency of 150 kHz, and a nominal tip radius of 8 nm. For the mechanical studies in fluid (distilled water), triangular silicon

https://doi.org/10.1021/acsomega.1c01576
ACS Omega 2021, 6, 15264−15273

nitride ScanAsyst Fluid cantilevers with a nominal spring constant of 0.7 N/m, a nominal frequency of 150 kHz, and a nominal tip radius of 20 nm were used. The real spring constants of the probes were measured by the thermal tune method. The deflection sensitivity was measured against a hard sapphire sample (Bruker, USA), and the real tip radii were estimated using a titanium roughness sample (Bruker, USA).

Ttopography images (10 × 10 μm) were obtained at a scan rate of 1 Hz and a resolution of 512 × 512 pixels in the PeakForce Tapping mode. The Young's moduli of the scaffolds on air and in water were mapped using the Fast Force Volume mode. On air, the force curves were acquired at an ≈7 μm/s vertical piezo speed up to the maximum force of 150 nN (indentation about 10 nm). In fluid, the force curves were acquired with an ≈9 μm/s vertical piezo speed and a maximum force of 5 nN; the first 40% of a force curve (indentation about 50 nm) after the contact point were used for the Young's modulus calculation. The force curve acquisition speed was 10 Hz, and 10 × 10 and 50 × 50 μm maps with a resolution of 16 × 16 and 32 × 32 pixels, respectively, were obtained. The Hertz model was used for the Young's modulus calculation. The mean value of the Young's modulus was calculated for each map and further averaged over five maps for each sample.

The data were processed using the NanoScope Analysis software version 1.9.

The diameter of SBEM fibers was measured based on AFM images using the NIH ImageJ freeware version 1.52n (Figure S1).

Scanning Electron Microscopy (SEM). Scanning electron microscopy was used to visualize the surface morphology of the SBEM. The hexamethyldisilazane (HMDS) drying method was used for sample dehydration. In brief, the mats were washed with PBS and subjected to dehydration with serial grades of ethanol. After the last step in absolute ethanol, samples were dipped in HMDS for 30 min followed by air-drying at room temperature for 24−36 h in a fume hood. Dried samples were mounted on aluminum stubs using double-sided conductive adhesive tape and visualized using a Phenom Pro X scanning electron microscope (LOT-QuantumDesign, The Netherlands).

Image Analysis and Data Processing. The length of neurites was measured using the "Annotations and measurements" modulus in the NIS Elements AR software package (Nikon). The estimation of the number of cells expressing one or several markers (SOX, βIII-tubulin, GFAP) was performed using flow cytometry with the subsequent processing in the Partec FloMax flow cytometry Data Acquisition and Analysis Software. An additional colocalization analysis and cell count of the substrate-fixed cell preparations was performed using NIS Elements AR.

All the experiments were performed in at least three independent runs to ensure the validity of the results. Data was presented as median, min, max, and 25% and 75% percentiles. Data with normal distribution were presented as mean ± standard deviation, and statistical significances for such data were calculated by the paired samples Student's *t*-test. One-way analysis of variance (ANOVA) was conducted using GraphPad Prism 9.0.0 software. The results with a *p*-value of <0.05 were considered statistically significant.

■ ASSOCIATED CONTENT

Supporting Information

The Supporting Information is available free of charge at https://pubs.acs.org/doi/10.1021/acsomega.1c01576.

(Table S1) The SBEM thickness; (Table S2) the results of the flow cytometry; (Table S3) fluorescence intensity by the Ivis Spectrum CT imager; (Figure S1) the diameter of fibers in different SBEM; (Figure S2) immunophenotyping of drNPCs after 10 days in the growth medium on spidroin-based electrospun mats with ECM peptide biomimetic motifs; (Figure S3) immunophenotyping of drNPCs after 14 days in the differentiation medium with BDNF and GDNF on spidroin-based electrospun mats with self-assembling peptide biomimetic motifs; (Figure S4) SBEM with or without the biotinylated motifs, incubated with Streptavidin DyLight488 (Vector Lab); (Figure S5) measurement of the fluorescence intensity of SBEM with or without biotinylated motifs using an Ivis Spectrum CT imager; (Figure S6) laser scanning confocal microscopy of SBEM-RGD vs TRITC and SBEM vs TRITC (PDF)

■ AUTHOR INFORMATION

Corresponding Author

Veronica A. Revkova − *Federal Research and Clinical Center of Specialized Medical Care and Medical Technologies FMBA of Russia, Moscow 115682, Russia;* orcid.org/0000-0003-0995-4620; Email: veronicarevkova@gmail.com

Authors

Konstantin V. Sidoruk − *National Research Center "Kurchatov Institute", Moscow 123182, Russia*

Vladimir A. Kalsin − *Federal Research and Clinical Center of Specialized Medical Care and Medical Technologies FMBA of Russia, Moscow 115682, Russia*

Pavel A. Melnikov − *Serbsky National Medical Research Center for Psychiatry and Narcology, Moscow 119034, Russia*

Mikhail A. Konoplyannikov − *Federal Research and Clinical Center of Specialized Medical Care and Medical Technologies FMBA of Russia, Moscow 115682, Russia; Institute for Regenerative Medicine, Sechenov First Moscow State Medical University, Moscow 119048, Russia*

Svetlana Kotova − *Institute for Regenerative Medicine, Sechenov First Moscow State Medical University, Moscow 119048, Russia; N. N. Semenov Federal Research Center for Chemical Physics, Russian Academy of Sciences, Moscow 119991, Russia*

Anastasia A. Frolova − *Institute for Regenerative Medicine, Sechenov First Moscow State Medical University, Moscow 119048, Russia*

Sergey A. Rodionov − *N. N. Priorov National Medical Research Center of Traumatology and Orthopedics, Moscow 127299, Russia*

Mikhail M. Smorchkov − *N. N. Priorov National Medical Research Center of Traumatology and Orthopedics, Moscow 127299, Russia*

Alexey V. Kovalev − *N. N. Priorov National Medical Research Center of Traumatology and Orthopedics, Moscow 127299, Russia*

https://doi.org/10.1021/acsomega.1c01576
ACS Omega 2021, 6, 15264−15273

Alexander V. Troitskiy − *Federal Research and Clinical Center of Specialized Medical Care and Medical Technologies FMBA of Russia, Moscow 115682, Russia*
Peter S. Timashev − *Institute for Regenerative Medicine, Sechenov First Moscow State Medical University, Moscow 119048, Russia; N. N. Semenov Federal Research Center for Chemical Physics, Russian Academy of Sciences, Moscow 119991, Russia; Chemistry Department, Lomonosov Moscow State University, Moscow 119991, Russia*
Vladimir P. Chekhonin − *Serbsky National Medical Research Center for Psychiatry and Narcology, Moscow 119034, Russia*
Vladimir G. Bogush − *National Research Center "Kurchatov Institute", Moscow 123182, Russia*
Vladimir P. Baklaushev − *Federal Research and Clinical Center of Specialized Medical Care and Medical Technologies FMBA of Russia, Moscow 115682, Russia*

Complete contact information is available at:
https://pubs.acs.org/10.1021/acsomega.1c01576

Notes

The authors declare no competing financial interest.

■ ACKNOWLEDGMENTS

The whole study was supported by the Russian Science Foundation (project no. 16-15-10432). The AFM studies were supported by the Russian Foundation for Basic Research (project no. 18-29-06059 mk). The sections of the recombinant spidroin biosynthesis and SBEM preparation were supported by an internal grant from the National Research Center Kurchatov Institute. The authors are grateful to Dr. Jan-Eric Ahlfors, the CEO of New World Laboratories, Inc. (Laval, QC), for kindly providing drNPCs. The authors signify their gratitude to Dr. Lyubov Davydova for her help in the spidroin biotinylation and labeling with TRITC.

■ REFERENCES

(1) Long, K. R.; Huttner, W. B. How the extracellular matrix shapes neural development. *Open biol* **2019**, *9*, 180216.
(2) Ahlfors, J. E.; Azimi, A.; El-Ayoubi, R.; Velumian, A.; Vonderwalde, I.; Boscher, C.; Mihai, O.; Mani, S.; Samoilova, M.; Khazaei, M.; et al. Examining the fundamental biology of a novel population of directly reprogrammed human neural precursor cells. *Stem Cell Res. Ther.* **2019**, *10*, 166.
(3) Takahashi, K.; Yamanaka, S. Induction of pluripotent stem cells from mouse embryonic and adult fibroblast cultures by defined factors. *Cell* **2006**, *126*, 663−676.
(4) Horisawa, K.; Suzuki, A. Direct cell-fate conversion of somatic cells: Toward regenerative medicine and industries. *Proc Jpn Acad Ser B Phys Biol Sci.* **2020**, *96*, 131−158.
(5) Karow, M.; Schichor, C.; Beckervordersandforth, R.; Berninger, B. Lineage-reprogramming of Pericyte-derived Cells of the Adult Human Brain into Induced Neurons. *J. Visualized Exp.* **2014**, *11*, 51433.
(6) Baklaushev, V. P.; Bogush, V. G.; Kalsin, V. A.; et al. Tissue Engineered Neural Constructs Composed of Neural Precursor Cells, Recombinant Spidroin and PRP for Neural Tissue Regeneration. *Sci. Rep.* **2019**, *9*, 3161.
(7) Revkova, V. A.; Grebenik, E. A.; Kalsin, V. A.; Demina, T. S.; Bardakova, K. N.; Shavkuta, B. S.; Melnikov, P. A.; Samoilova, E. M.; Konoplyannikov, M. A.; Efremov, Y. M.; et al. Chitosan-*g*-oligo(L,L-lactide) Copolymer Hydrogel Potential for Neural Stem Cell Differentiation. *Tissue Eng Part A* **2020**, *26*, 953−963.
(8) Debabov, V. G.; Bogush, V. G. Recombinant Spidroins as the Basis for New Materials. *ACS Biomater. Sci. Eng.* **2020**, *6*, 3745−3761.
(9) Hinman, M. B.; Jones, J. A.; Lewis, R. V. Synthetic spider silk: a modular fiber. *Trends Biotechnol.* **2000**, *18*, 374−379.
(10) Bowen, C. H.; Dai, B.; Sargent, C. J.; Wenqin Bai, W.; Ladiwala, P.; Feng, H.; Huang, W.; Kaplan, D. L.; Galazka, J. M.; Zhang, F. Recombinant Spidroins Fully Replicate Primary Mechanical Properties of Natural Spider Silk. *Biomacromolecules* **2018**, *19*, 3853−3860.
(11) Hersel, U.; Dahmen, C.; Kessler, H. RGD modified polymers: biomaterials for stimulated cell adhesion and beyond. *Biomaterials* **2003**, *24*, 4385−4415.
(12) Mauri, E.; Sacchetti, A.; Vicario, N.; Peruzzotti-Jametti, L.; Rossi, F. Pluchino S Evaluation of RGD functionalization in hybrid hydrogels as 3D neural stem cell culture systems. *Biomater. Sci.* **2018**, *6*, 501−510.
(13) Matsuda, A.; Kobayashi, H.; Itoh, S.; Kataoka, K.; Tanaka, J. Immobilization of laminin peptide in molecularly aligned chitosan by covalent bonding. *Biomaterials* **2005**, *26*, 2273−2279.
(14) Ji, W.; Álvarez, Z.; Edelbrock, A. N.; Sato, K.; Stupp, S. I. Bioactive Nanofibers Induce Neural Transdifferentiation of Human Bone Marrow Mesenchymal Stem Cells. *ACS Appl. Mater. Interfaces* **2018**, *10*, 41046−41055.
(15) Ahmed, I.; Liu, H. Y.; Mamiya, P. C.; Ponery, A. S.; Babu, A. N.; Weik, T.; Schindler, M.; Meiners, S. Three-dimensional nanofibrillar surfaces covalently modified with tenascin-C-derived peptides enhance neuronal growth in vitro. *J Biomed Mater Res A.* **2006**, *76*, 851−860.
(16) Berns, E. J.; Álvarez, Z.; Goldberger, J. E.; Boekhoven, J.; Kessler, J. A.; Kuhn, H. G.; Stupp, S. I. A tenascin-C mimetic peptide amphiphile nanofiber gel promotes neurite outgrowth and cell migration of neurosphere-derived cells. *Acta Biomater.* **2016**, *37*, 50−58.
(17) Balion, Z.; Cėpla, V.; Svirskiene, N.; Svirskis, G.; Druceikaitė, K.; Inokaitis, H.; Rusteikaitė, J.; Masilionis, I.; Stankevičienė, G.; Jelinskas, T.; et al. Cerebellar Cells Self-Assemble into Functional Organoids on Synthetic, Chemically Crosslinked ECM-Mimicking Peptide Hydrogels. *Biomolecules* **2020**, *10*, 754.
(18) Ruan, H.; Xiao, R.; Jiang, X.; Zhao, B.; Wu, K.; Shao, Z.; Zhang, Z.; Duan, H.; Song, Y. Biofunctionalized self-assembly of peptide amphiphile induces the differentiation of bone marrow mesenchymal stem cells into neural cells. *Mol. Cell. Biochem.* **2019**, *450*, 199−207.
(19) Farrukh, A.; Zhao, S.; Paez, J. I.; Kavyanifar, A.; Salierno, M.; Cavalié, A.; Del Campo, A. In Situ, Light-Guided Axon Growth on Biomaterials via Photoactivatable Laminin Peptido mimetic IK-(HANBP)VAV. *ACS Appl. Mater. Interfaces* **2018**, *10*, 41129−41137.
(20) Farrukh, A.; Fan, W.; Zhao, S.; Salierno, M.; Paez, J.; Del Campo, A. Photoactivatable Adhesive Ligands for Light-Guided Neuronal Growth. *ChemBioChem* **2018**, *19*, 1271−1279.
(21) Faissner, A.; Roll, L.; Theocharidis, U. Tenascin-C in the matrisome of neural stem and progenitor cells. *Mol Cell Neurosci.* **2017**, *81*, 22−31.
(22) May, M.; Denecke, B.; Schroeder, T.; Götz, M.; Faissner, A. Cell tracking in vitro reveals that the extracellular matrix glycoprotein Tenascin-C modulates cell cycle length and differentiation in neural stem/progenitor cells of the developing mouse spinal cord. *Biol Open.* **2018**, *7*, bio027730.
(23) Katsamakas, S.; Chatzisideri, T.; Thysiadis, S.; Sarli, V. RGD-mediated delivery of small-molecule drugs. *Future Med. Chem.* **2017**, *9*, 579−604.
(24) Macková, H.; Plichta, Z.; Proks, V.; Kotelnikov, I.; Kučka, J.; Hlídková, H.; Horák, D.; Kubinová, Š.; Jiráková, K. RGDS- and SIKVAVS-Modified Superporous Poly (2-hydroxyethyl methacrylate) Scaffolds for Tissue Engineering Applications. *Macromol. Biosci.* **2016**, *16*, 1621−1631.
(25) Tang-Schomer, M. D. 3D axon growth by exogenous electrical stimulus and soluble factors. *Brain Res.* **2018**, *1678*, 288−296.
(26) Rozario, T.; DeSimone, D. W. The extracellular matrix in development and morphogenesis: a dynamic view. *Dev. Biol.* **2010**, *341*, 126−140.
(27) Li, X.; Shi, C.-H.; Tang, C.-L.; Cai, Y.-M.; Meng, Q. The correlation between the length of repetitive domain and mechanical

properties of the recombinant flagelliform spidroin. *Biol Open.* **2017**, *6*, 333−339.
(28) Finnigan, W.; Roberts, A. D.; Ligorio, C.; Scrutton, N. S.; Breitling, R.; Blaker, J. J.; Takano, E. The effect of terminal globular domains on the response of recombinant mini-spidroins to fiber spinning triggers. *Sci. Rep.* **2020**, *10*, 10671.
(29) Pereira, M.; Birtele, M.; Ottosson, R. D. Direct reprogramming into interneurons: potential for brain repair. *Cell. Mol. Life Sci.* **2019**, *76*, 3953−3967.
(30) Zhao, J.; Santino, F.; Giacomini, D. Luca Gentilucci Integrin-Targeting Peptides for the Design of Functional Cell-Responsive Biomaterials. *Biomedicines.* **2020**, *8*, 307.
(31) Hosoyama, K.; Lazurko, C.; Muñoz, M.; McTiernan, C. D.; Alarcon, E. I. Peptide-Based Functional Biomaterials for Soft-Tissue Repair. *Front Bioeng Biotechnol.* **2019**, *7*, 205.
(32) Ramo, N. L.; Troyer, K. L.; Puttlitz, C. M. Viscoelasticity of spinal cord and meningeal tissues. *Acta Biomater.* **2018**, *75*, 253−262.
(33) Romano, N. H.; Madl, C. M.; Heilshorn, S. C. Matrix RGD ligand density and L1CAM-mediated Schwann cell interactions synergistically enhance neurite outgrowth. *Acta Biomater.* **2015**, *11*, 48−57.
(34) Stukel, J. M.; Willits, R. K. The interplay of peptide affinity and scaffold stiffness on neuronal differentiation of neural stem cells. *Biomed Mater.* **2018**, *13*, No. 024102.
(35) Sidoruk, K. V.; Davydova, L. I.; Kozlov, D. G.; Gubaidullin, D. G.; Glazunov, A. V.; Bogush, V. G.; Debabov, V. G. Fermentation optimization of a Saccharomyces cerevisiae strain producing 1F9 recombinant spidroin. *Appl. Biochem. and Microbiol.* **2015**, *51*, 766−773.
(36) Nagoshi, N.; Khazaei, M.; Ahlfors, J. E.; Ahuja, C. S.; Nori, S.; Wang, J.; Shibata, S.; Fehlings, M. G. Human Spinal Oligodendrogenic Neural Progenitor Cells Promote Functional Recovery After Spinal Cord Injury by Axonal Remyelination and Tissue Sparing. *Stem Cells Transl Med.* **2018**, *7*, 806−818.

https://doi.org/10.1021/acsomega.1c01576
ACS Omega 2021, 6, 15264−15273